JOURNAL OF OPTOELECTRONICS AND ADVANCED MATERIALS Vol. 12, No. 3, March 2010, p. 589 - 594

Generation of Ce and W doped titanium oxide thin films by pulsed excimer laser irradiation

YASIR F. JOYA*, ZHU LIU
Corrosion & Protection Centre, The Mill, School of Materials, The University of Manchester, Manchester, M60 1QD, United Kingdom

Mesoporous (pore size<50 nm) anatase and rutile based films were generated in WO_3 doped TiO_2 films by excimer laser induced transformation. CeO_2 (5 wt.%) and WO_3 (3 wt.%) doped TiO_2 precursor films were prepared by a sol-gel method and spin-coated on Pt(Si) substrate. KrF (248 nm, 13 ns) pulsed excimer laser beam with variation in fluence and number of pulses, was applied on film surface. The effect of laser operating conditions on TiO_2 crystallization, microstructure and morphology was studied by Raman spectroscopy, FEG-SEM and AFM respectively. Anatase was revealed at laser fluence of 35mJ/cm^2 in both TiO_2 compositions. Ce doped film was crystallized to anatase under higher number of laser pulses in contrast to W doped TiO_2. Whereas, finer features and surface morphology was obtained in the later.

(Received June 30, 2009; accepted December 3, 2009)

Keywords: Pulsed excimer laser, Sol-gel, Anatase, Raman Spectroscopy, Laser Induced Phase transformation, FEG-SEM

1. Introduction

Titanium dioxide, or titania (TiO_2) is a well known transition metal oxide due to its stability, low cost, non-toxicity and applications in photocatalysis, self-cleaning surfaces, antibacterial coatings, gas sensors, organics decomposition and water purification etc. [1-3]. TiO_2 exists in three polymorphs namely brookite (orthorhombic), anatase (tetragonal), and rutile (tetragonal) respectively of which anatase is the most desired phase because of its highest photo-activity and anti-bacterial properties [4, 5]. However, anatase has a wider band gap (3.2 eV) and thus absorb light with wavelength of 385 nm and below to activate water molecules to create strongly oxidizing hydroxyl (OH) radicals and strongly reducing dioxygen ions (O^{2-})[6]. It is also unstable above 450°C and transforms to a stable rutile phase [7]. This phase transition is undesirable for most applications and may be suppressed to some extent by optimizing preparation conditions and addition of impurities/dopants etc. [8]. The addition of lanthanides has shown considerable enhancement in stabilizing anatase and enhanced photocatalysis of titania [9, 10]. Among lanthanides, CeO_2 has shown significant results to control the stability of anatase at higher temperatures [11,12]. Besides, WO_3 may serve dual purpose in stabilizing anatase as well as enhancing the photocatalysis in TiO_2 [13].

A plethora of research has been devoted to prepare TiO_2 nanoparticles and films with diverse microstructures to improve the photocatalysis and other properties of interest [3,6,14]. It is believed that increasing TiO_2 surface area by fabricating anatase mesoporous films, photocatalytic behavior would be improved [15,16]. Generally, sol-gel method is used to fabricate mesoporous TiO_2 films by using cationic surfactants or copolymer templates as structuring agents [17, 18]. Conventional heat treatment of sol-gel derived oxide films in furnaces has a major drawback of localized film-substrate interactions resulting in defected films hence making their deposition on substrates like plastics and polymers very difficult.

Lasers find widespread applications today from characterizations to the preparation, and processing of a variety of materials to various forms [19]. Recently, annealing/crystallization of the sol-gel metal oxide precursor films by using lasers has shown promising results [20-23]. It is necessary to mention that crystallization of sol-gel derived films by continuous wave (cw) laser annealing such as CO_2 (10.6 μm) and/or Nd:YAG (1.06 μm) may be ascribed to thermal effects. Whereas, ultraviolet (UV) pulsed excimer laser keeps a high photon energy (0.248 μm) coupled with nanosecond pulse width. As a result, excimer laser beam induces non-thermal modifications in sol-gel film due to the photochemical effect [24]. In addition, thermal effect caused by the high energy laser beam is responsible for phase transformation between the amorphous, atanase and rutile respectively. It is assumed that as anatase phase crystallizes out of amorphous titania during laser irradiations, its absorbance to UV photons may increase resulting in the transformation into rutile phase instantaneously. With visible and infrared lasers (Nd:YAG, CO_2) operating in cw mode and lower photon energy, the process flexibility is limited. Nevertheless, pulsed excimer laser offers more to process sol-gel thin films on any kind of substrate.

In continuation to our previous work [25], this paper, reports on a single-step process using a KrF laser to crystallize sol-gel prepared Ce and W ions doped TiO_2 thin films respectively. These dopant ions were added with the aim to study their effect on phase transformation and the microstructure of titania films.

2. Experimental

Two types of TiO_2 precursor films were prepared by sol-gel method. The first composition was doped with 5

wt. % CeO_2 and the other with 3 wt. % WO_3 respectively. In both compositions, titanium n-butoxide $Ti(C_4H_9O)_4$ was used as the TiO_2 precursor, cerium nitrate $Ce(NO_3)_2$, acetic acid (CH_3COOH), n-butanol (C_4H_9OH) and de-ionised (DI) water to prepare a cerium modified TiO_2 precursor sol-gel system. The molar ratio of $Ti:CH_3COOH:H_2O$ was selected as 1:2:2. The WTO sol-gel films were prepared with same precursors/solvents as above with the addition of tungsten (VI) isopropoxide $W(iPr)_6$ as the WO_3 precursor inplace of $Ce(NO_3)_2$. Cerium and tungsten doped titanium oxide film may be named as CTO and WTO respectively hereafter for brevity. Moreover, pure titania precursor sol-gel batch was also prepared without any doping additions.

The chemicals were mixed stepwise while magnetically stirred overnight at room temperature. This step gave a 0.36 Molar Ti sol for subsequent spin coating. The sol-gel solutions were aged at room temperature for 24 hours in a sealed beaker. Later the films were deposited on Pt coated Si (100) substrate by spin coating method. Each sample was prepared by coating up to four consecutive layers of TiO_2 precursor sol while each layer was dried at 300°C for 2 minutes. The drying step was necessary to evaporate free volatiles and to decompose the organic species inside the sol-gel film. This led to a TiO_2 precursor film in a dried amorphous state before laser processing.

The dried films were subjected to Lumonics PM-840 KrF excimer laser (λ=248 nm, pulse width=13 ns) using a wide range of laser operating parameters. Typically, laser fluence was varied from 35-45 mJ/cm^2 and up to 800 number of pulses, were used. It must be noted that in all experiments the laser repetition rate was set to be 10 Hz. The samples were moved across the stationary laser beam in x-y to cover approximately 1x1cm^2 area.

The laser processing was carried at ambient atmosphere. The laser beam was masked through 0.5x0.5 cm^2 and de-focused onto the work piece in order to obtain a uniform energy distribution over the film surface. Laser fluence was varied between 25-50 mJ/cm^2 and the number of laser pulses up to 500 at a fixed pulse repetition rate of 10 Hz. The parameters were varied keeping at least one constant to study their effect on film transformation. Laser irradiated films were characterized against their structural changes by using Ar ion laser (512 nm) Raman spectroscopy. Raman spectra were recorded in the range of 100-1000 cm^{-1} with accumulation time of 10-20 seconds. The microstructural features were imaged using a Field emission gun scanning electron microscope (FEG-SEM). The film thickness and 3-D surface profile were measured using an atomic force microscope (AFM).

3. Results and discussion

3.1 Raman spectroscopy of CTO and WTO films

Fig. 1(a-d) compares the Raman spectra from CTO and WTO films treated by laser at various parameters i.e. laser fluence, number of pulses etc. Both of the films revealed amorphous structure in the as dried state (before laser irradiation) as shown in Fig. 1a and 1b respectively. CTO films were irradiated first by excimer laser beam at 35 mJ/cm^2 fluence for 100 pulses respectively. Anatase as a dominant phase was identified after analyzing by Raman spectrum as shown in Figure 1a. However a small shoulder from rutile peak was also evident. The CTO film irradiated at a higher laser fluence of 45 mJ/cm^2 and 100 pulses, indicated rutile phase from Raman spectrum in Figure 1a. Therefore indicate that increasing the laser fluence has a direct effect on phase transformation from anatase to rutile[26]. As anatase is a metastable phase it can be converted to rutile by experiencing higher laser fluence at the same number of pulses. It may be inferred that by increasing laser fluence, the peak temperature produced by excimer laser pulse interaction with CTO film would subsequently increase.

On the other hand, WTO films were laser irradiated at the same operating conditions and results obtained are shown by Raman spectra in Figure 1b. Excimer laser irradiation of WTO film at 35 mJ/cm^2 with 100 laser pulses formed anatase and rutile combined phase as shown in Fig. 1(b). However the peaks were rather weak as compared to the CTO film. The WTO film laser irradiated at 45 mJ/cm^2 was partially converted to rutile phase as shown in Figure 1b. The phase transformation from amorphous to anatase and then to rutile in WTO was different as compared to CTO film. In order to study this phenomenon, WTO films were irradiated with excimer laser keeping the fluence fixed at 35 mJ/cm^2. The number of laser pulses was varied from 10-100. Results obtained were quite surprising as only 10 laser pulses (processing time=1 second) crystallized WTO film to anatase as shown in Fig. 1d. As the pulses were increased from 50 to 100, additional peaks from rutile appeared in Raman spectra indicating the meta-stability of anatase. Most of anatase was converted to rutile phase after 100 laser pulses as shown in Fig. 1d. It may be noted that the samples results shown in Figure 1b and 1d look a bit different from each other. The reason for this behavior may be due to pulse to pulse energy variation from the laser at different spots on film.

CTO films on the other hand, exhibited a dissimilar behavior against transformation. Laser pulses below 100 did not show any major effect on CTO films. The laser pulses were increased upto 800 at a fixed fluence of 35 mJ/cm^2 with a pulse repetition rate of 10 Hz respectively. The sample irradiated at 100 pulses produced crystalline anatase as shown in Fig. 1c. The peaks intensity of anatase was increased with increasing laser pulses up to 500 but rutile also appeared as shown in Figure 1c. Further laser irradiation up to 800 pulses gave mixed anatase and rutile phases. These results may be attributed to Ce ions activity in hindering the phase transformation from anatase into rutile [12]. The results indicated that CTO required greater number of laser pulses for crystallization as compared to WTO.

The Raman spectra results indicated a relationship among phase transformation, laser fluence and the number of pulses.

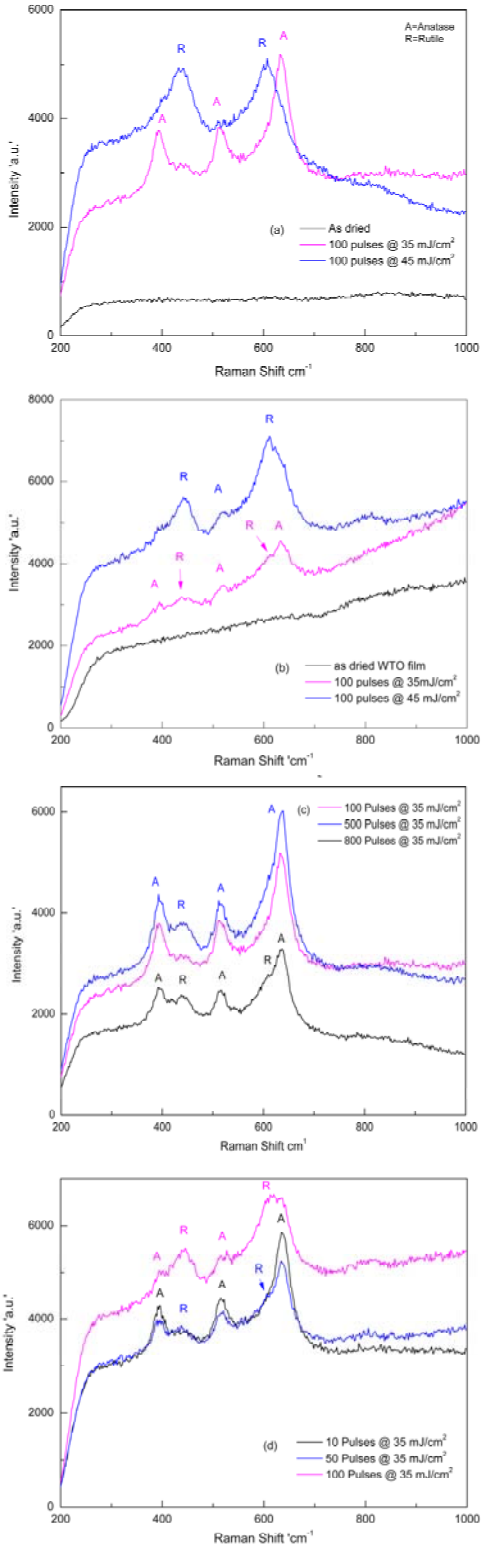

Fig. 1. Raman spectra of CTO (a, c) and WTO (b, d) laser irradiated films at various parameters.

Increasing the number of laser pulses, irradiation time of the film is increased from 10 seconds at 100 pulses to 80 seconds at 800 pulses respectively which lead to the formation of rutile. However, laser irradiation time should not be associated with the laser interaction time which is derived from the laser pulse width (13 ns).

3.2 FEG-SEM Imaging

SEM image obtained from the as dried CTO and WTO films is shown in Figure 2a and 2d respectively. Those appeared featureless with a flat surface. However, after laser irradiation for 100 pulses at 35 mJ/cm^2, CTO film roughness increased and a new microstructure was obtained as shown in Figure 2b. In addition, CTO film was mesoporous as shown by the inset (scale bar=500nm) in Figure 2b which is a magnified image of the same sample. The average pore size measured by SEM line marking was 38 nm. The meso-porosity may be produced during laser irradiation as a result of decomposition of the remaining organic constituents in the film.

As the laser fluence was increased up to 45 mJ/cm^2, CTO film revealed a coarse surface morphology after receiving 100 pulses as shown in Figure 2e. Earlier, Raman results identified rutile phase in the same sample. It may be inferred that the laser fluence was high enough to cross the anatase phase boundary and transformed it to rutile with larger surface features. This is because rutile is formed after anatase grains coalesce and grow in size by receiving energy/heat from the incident laser beam. The pores may also be seen as retained in the image after laser treatment and the pore size was also increased.

On the other hand, SEM image in Figure 2b was taken from WTO film surface before laser irradiation. Figure 2d shows the microstructure obtained after laser treatment at 35 mJ/cm^2 and 100 pulses. A uniform fine grained microstructure was observed. In addition, a mesoporous structure similar to the CTO sample was also indicated by sample. The pore size obtained from SEM was 34 nm. Anatase and rutile mixed phases were identified earlier by Raman spectroscopy from the sample. As laser fluence was increased up to 45 mJ/cm^2, the microstructure was changed to a coarser one after receiving 100 pulses as shown in Figure 2f. Again, this was result of the formation of a denser phase i.e. rutile. The features were smaller in size as compared to a similar CTO sample. The actual science involved is not very clear yet as many factors may be involved such as film composition, optical effect of W ions in TiO_2 lattice etc. Further experiments are required to explore this mechanism.

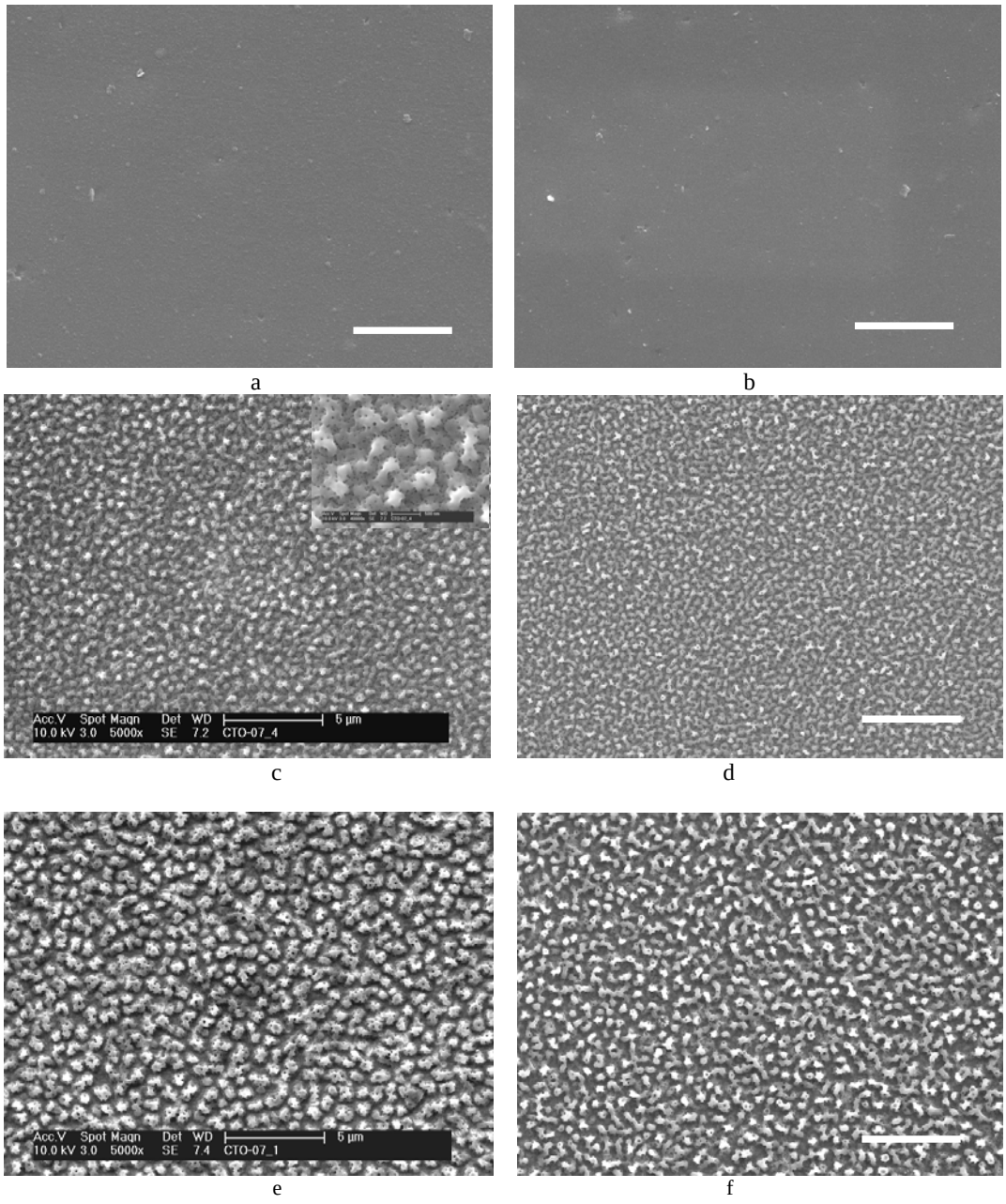

Fig. 2. FEG-SEM images of as dried and laser irradiated films at 35 and 45 mJ/cm2 for 100 pulses from CTO (a,c,e) and WTO (b,d,f) batches respectively (scale bar=5µm).

3.3 AFM Surface Analysis

Surface profiles of CTO and WTO films were measured by using AFM three-dimensional imaging. The image and histogram obtained from laser irradiated CTO film at 35 mJ/cm^2 for 100 pulses, are shown in Fig. 3a. The surface revealed a near spherical morphology and a quite uniform distribution in three dimensions. Average feature size was less than 200 nm in x and y directions, and less than 100 nm in z direction respectively.

On the other hand, laser irradiated at the same parameters, WTO film exhibited finer features as shown in Fig. 3b. The surface features were smaller in geometry as compared to CTO films and exhibited agglomerated particles. The average feature size was less than 100 nm in x and y axis and about 55 nm in z axis respectively.

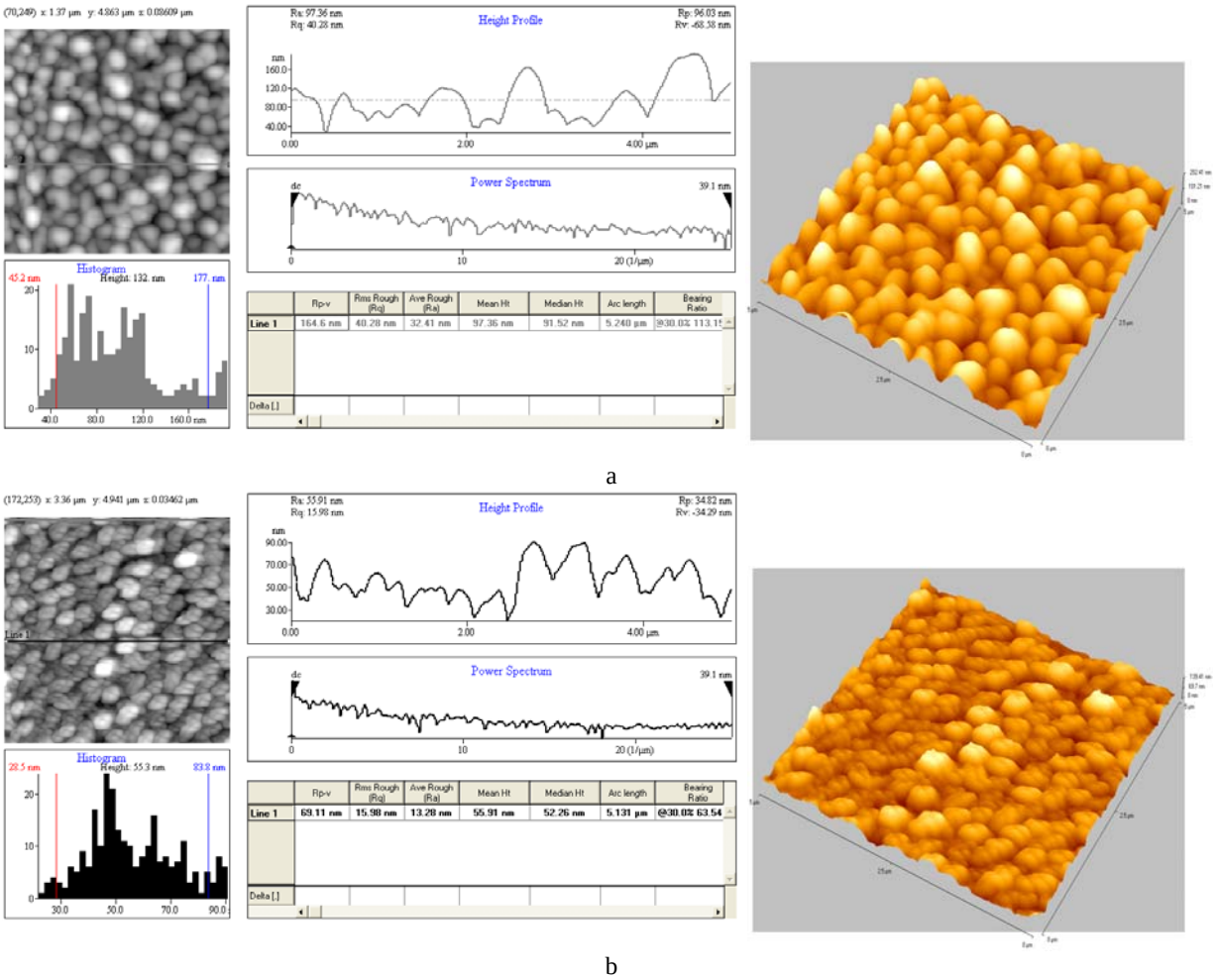

Fig. 3. AFM 3-D surface profile obtained from laser irradiated for 100 pulses at 35 mJ/cm^2 CTO a) and WTO b) film. (scale bar=1μm) .

4. Conclusions

Anatase and rutile based TiO_2 thin films were successfully synthesized by a single-step pulsed excimer laser irradiation. CeO_2 and WO_3 additions to TiO_2 produced fine features and mesoporous anatase without any template addition to the sol-gel. Anatase phase was achieved by optimizing the laser fluence and the number of pulses applied. A uniform distribution of grains after laser processing was demonstrated by the films. WTO yielded finer features as compared to CTO. Experiments on photocatalytic performance of these films would be important for their evaluation and is underway.

Acknowledgements

The authors would gratefully like to acknowledge Higher Education Commission (HEC) Pakistan, as the main sponsor and Northwest Science Council through Northwest Laser Engineering Consortium (NWLEC), UK for their partial financial support in this project.

References

[1] A. Fujishima, K. Honda, Nature, **238,** 37 (1972).
[2] B. O'Regan, M. Gratzel, Nature, **353,** 737 (1991).
[3] X. Chen and S.S. Mao, Chemical Reviews, **107,** 2891 (2007).
[4] T. I. N. Negishi, K. Hashimoto and A. Fujishima, Chem. lett. 841 (1995) .
[5] T. I. Y. Kikushi, K. Hashimoto and A. Fujishima, J. Photochem. Photobiol. A, **106,** 51 (1997).
[6] A. L. Linsebigler, G. Lu, and J.T. Yates, Chemical Reviews **95,** 735 (1995).
[7] S. R. Yoganarasimhan and C.N.R. Rao, Trans. Faraday Soc. **58,** 1579 (1962) .
[8] M. Hirano, C. Nakahara, K. Ota, O. Tanaike, M. Inagaki, Journal of Solid State Chemistry **170,** 39 (2003).
[9] C. A. LeDuc, J. M. Campbell, J. A. Rossin, Industrial & Engineering Chemistry Research, **35,** 2473 (1996).

[10] A. Burns, G. Hayes, W. Li, J. Hirvonen, J. D. Demaree, S.I. Shah, Materials Science and Engineering B **111** 150 (2004).
[11] P. Periyat, K. V. Baiju, P. Mukundan, P. K. Pillai, K. G. K. Warrier, Journal of Sol-Gel Science and Technology **43** 299 (2007).
[12] Y.-h. Xu, H.-r. Chen, Z.-x. Zeng, B. Lei, Applied Surface Science **252,** 8565 (2006).
[13] X. Z. Li, F. B. Li, C. L. Yang, W. K. Ge, Journal of Photochemistry and Photobiology A: Chemistry **141,** 209 (2001).
[14] M. M. Yusuf, H. Imai, H. Hirashima, Journal of Non-Crystalline Solids, **285,** 90 (2001).
[15] H. S. Yun, K. Miyazawa, H. S. Zhou, I. Honma, M. Kuwabara, Advanced Materials, **13,** 1377 (2001).
[16] M. Wark, J. Tschirch, O. Bartels, D. Bahnemann, J. Rathouský, Microporous and Mesoporous Materials **84,** 247 (2005).
[17] X. S. Li, G. E. Fryxell, J. C. Birnbaum, C. Wang, Langmuir, **20,** 9095 (2004).
[18] F. Bosc, A. Ayral, P.-A. Albouy, C. Guizard, Chemistry of Materials, **15,** 2463 (2003).
[19] J. C. Ion, Laser Processing of Engineering Materials, principles, procedure and industrial application, Elsevier Butterworth-Heinemann, Oxford, 1st ed., 2005, pp. 2.
[20] D. J. Taylor, B. D. Fabes, Journal of Non-Crystalline Solids, **147-148,** 457 (1992).
[21] M. R. S. Castro, E. D. Sam, M. Veith, P. W. Oliveira, Nanotechnology, **19,** 105704 (2008).
[22] T. Tsuchiya, A. Watanabe, H. Niino, A. Yabe, I. Yamaguchi, T. Manabe, T. Kumagai, S. Mizuta, Applied Surface Science, **186,** 173 (2002).
[23] T. F. Naoko Asakuma, Mamoru Aizawa, Motoyuki Toki, Hiroaki Imai, Hiroshi Hirashima, Journal of Sol-Gel Science and Technology, **19,** 333 (2000).
[24] D. Bauerle, Laser Processing and Chemistry Springer-Verlag, Heidelberg Berlin 3rd ed., 2000, p.13.
[25] Y. F. Joya, Z. Liu, Scripta Materialia **60,** 467 (2009).
[26] H. Sato, S. Nishio, S. Kato, K. Marumo, A. Matsuzaki, R. Yoshida, Bulletin of the Chemical Society of Japan **69** 3381 (1996).

*Corresponding author: yasir.joya@postgrad.manchester.ac.uk